Direct numerical simulation of primary break-up in swirling liquid jets

Claudio Galbiati[1], Simona Tonini[1]*, Bernhard Weigand[2] and Gianpietro E. Cossali[1]

[1] *University of Bergamo*
Viale Marconi 2, Dalmine (BG), Italy

[2] *University of Stuttgart*
ITLR, Pfaffenwaldring 31, 70569 Stuggart, Germany

**Corresponding author: simona.tonini@unibg.it*

Abstract

The development and fragmentation of a conical swirled liquid jet has been numerically predicted implementing a multi-phase flow model according to the VOF (Volume Of Fluid) methodology. Direct numerical simulations (DNS) have been performed using the in-house FS3D (Free Surface 3D) code. Two operating conditions, corresponding to typical test cases for an aircraft engine, have been investigated under isothermal and non reacting environment. The inlet boundaries of the numerical problem, corresponding to the characteristics of the annular liquid lamella at the nozzle exit and the internal air core, have been provided by previous internal nozzle flow calculations based on LES (Large Eddy Simulation) methodology. The main features of the jet evolution and fragmentation are analysed, evaluating the lamella instability characteristics in terms of fastest growing wavelength and break-up length. The break-up outcomes are liquid ligaments, which shape and size were evaluated and statistically described. Comparison with available analytical models are reported and discussed.

Keywords: DNS, conical swirled jet, primary break-up.

1. Introduction

Conical swirled jets from Pressure Swirl Atomizers (PSAs) are commonly used in several industrial fields to generate finely atomised sprays. PSAs have the peculiarity to work at a relatively low feeding system pressure and have a simple geometry, which means simple manufacturing, but with a good quality of the final spray [1]. Investigation on the jet development and break-up is needed to clearly understand how to control spray characteristics. As an example, in the combustion field the control of the droplet dimension allows to partially control the chemical reactions, and then the production of pollutants (in particular NOx for aero-engines).

The break-up of liquid jets is in general divided into two stages: primary and secondary break-up. The first one is the phenomenon that leads to the rupture of the liquid jet and to the formation of liquid ligaments and droplets; the secondary break-up comprises a collection of phenomena that are responsible of the subsequent atomisation mechanism to yield the final spray [ref]. For the primary break-up, a limited amount of experimental data is available, mainly due to the intrinsic limitations of the commonly used experimental techniques for spray characterization, like Phase or Laser Doppler Anemometry (PDA and LDA), or Particle Image Velocimetry (PIV). Several analytical models were developed in the past to predict the characteristics of the jet evolution and break-up characteristics and of the primary drops, like the models of Senecal at al. [2] and Panchangula et al. [3] (see [4] for further details about the unstable wave propagation over the liquid jet surface). However, more data on the atomization mechanism are needed to validate all the assumptions. In the recent years many researchers, thanks to the increased computational power that became available, tackled the problem by Direct Numerical Simulation (DNS) of the liquid-gas interface evolution and break-up. Different authors performed multiphase numerical simulations of round [5-7] and planar jets [8], while the case of conical jets, to the best of the Authors' knowledge, has not been investigated yet. This work is then aimed to provide additional information on the development and primary beak-up of a conical swirled liquid jet by performing multiphase DNS, using the in-house Free Surface 3D (FS3D) solver.

2. Numerical set-up

FS3D is a finite volume multiphase DNS solver for incompressible fluids. The incompressible flow is governed by the conservation equations for mass and momentum:

$$\frac{\partial \rho}{\partial t} + \nabla \cdot \left(\rho u \right) = 0 \tag{1}$$

$$\frac{\partial \left(\rho u \right)}{\partial t} + \nabla \cdot \left(\rho u u \right) = \nabla \cdot \left[S - Ip \right] + \rho g + f_\sigma \tag{2}$$

see the nomenclature section for the meaning of the symbols. The Volume of Fluid (VOF) model [9] is adopted to follow the liquid jet development into the quiescent gas. More detailed information on FS3D can be found in [9].

2.1. Inlet boundary

The inlet boundary comprises an annular inlet region, where the liquid injection velocity is imposed, and an inner circle, where the gas velocity is set to represent the air-core, refer to Figure 2 for more details. The value of the liquid film thickness (*2h*) at inlet is defined by the outcomes of a previous numerical analysis (RANS- and LES-VOF simulations) of the internal nozzle flow in a PSA for aeronautical applications [7]. Also the

*Footnotes may appear on the first page only to indicate research grant, sponsoring agency, etc. These should not be numbered but referred to by symbols, e.g. *,+. The footnote text may be produced in a small font.

liquid velocity profile at inlet was set on the basis of the same simulations, see Figure 1.

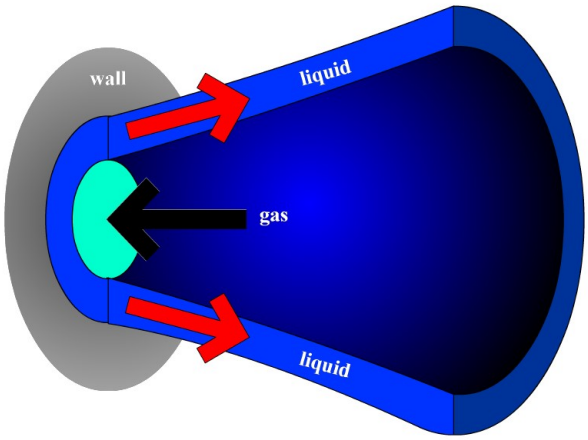

Figure 1: Sketch of inlet boundaries and liquid and gas regions.

To check the influence of the inlet velocity on the outcomes, numerical simulations were also performed using a simplified velocity profile, where the liquid and gas velocities are uniformly distributed (conserving the flow rate values) over the annular and circular sections [7]. The comparison showed that the inlet velocity distributions significantly influence the jet evolution, then the following analysis was done using the above mentioned more realistic profile (Figure 2).

2.2. Geometry and grid generation

The computational domain is reported in Figure 3: the inlet boundaries are located at the centre of the left hand side wall, while on the remaining part no-slip conditions are imposed. A continuous (Neumann) boundary condition is set on the other boundaries. The nozzle diameter (d_0) (equal to 625 µm) is used to define the dimension of the whole computational domain: to balance between a reasonable numerical effort and the necessary space for a correct jet evolution the linear dimensions of the computational domain is set equal to $10.5d_0$ along the transversal directions (y and z, as shown in Figure 3), and $7.5d_0$ along the axis of the jet. The size of the computational domain was chosen to minimise the boundary effects on the simulation outcomes.

A DNS simulation requires a grid cell size of the order of the Kolmorogov length scale [10], which is defined as follows:

$$\lambda_k = \frac{L_t}{\mathrm{Re}_t^{3/4}} \tag{3}$$

$$\mathrm{Re}_t = \frac{\rho_l \sqrt{u'^2}\, L_t}{\mu_l} \tag{4}$$

where L_t is the macro-scale turbulence length, which in the present investigation is set equal to *2h/10* [10]; Re_t is the turbulence Reynolds number, which depends on the average turbulent velocity fluctuations at the exit section of the atomizer, extracted from the above mentioned simulations of the internal nozzle flow [11].

A grid independence investigation, reported in [10], suggested that a grid cell size approximately 8 times larger than the Kolmogorov scale is a reasonable compromise between the required numerical effort and an acceptable accuracy of the predictions.

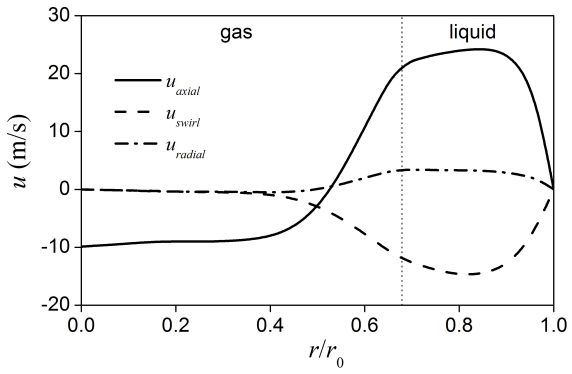

Figure 2: Radial velocity profiles at nozzle exit for case # 1 listed in Table 1.

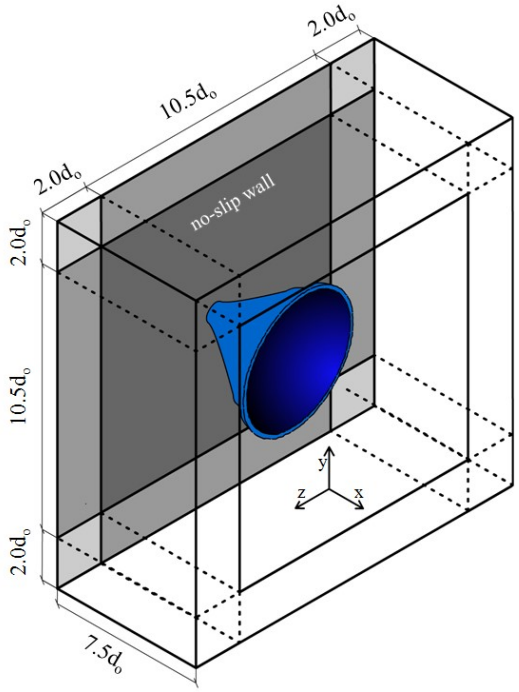

Figure 3: Dimensions of computational domain.

2.3. Test cases

Two operation conditions were investigated, corresponding to take off 50% and approach 30% conditions [11]; the main difference between the two cases is related to the gas density, see Table 1 for further details. The performed simulations are non-reacting and isothermal and the properties of both fluids are kept constant. The liquid properties are those of Kerosene Jet A-1: density, viscosity and surface tension are taken equal to ρ_l = 799kg/m^3, μ_l = 0.0013Pas and σ = 0.0224N/m.

Test case	-	$\dot{m}_l \times 10^3$ [kg/s]	ρ_g [kg/m^3]	$2h$ [µm]	KF	n_{cell} $\times 10^8$
# 1	Take off 50%	2.8	13.3	100.4	8.4	3.03
# 2	Approach 30%	3.0	6.8	94.6	8.6	5.37

Table 1: Investigated operating conditions and computational grid characteristics.

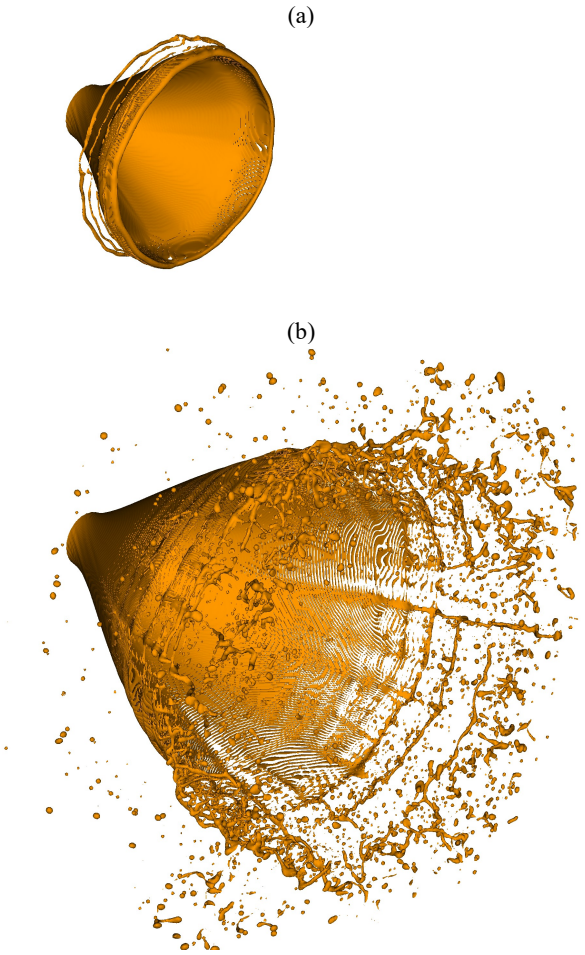

Figure 1: Jet development and spray formation at (a) 0.1 ms and (b) 0.3 ms after the start of injection, for case #1 of Table 1.

3. Results

Figure 4 shows a sketch of the jet development as it exits the discharge nozzle at 0.1 and 0.3 ms after start of injection, evidencing the opening of the liquid lamella according to the umbrella-type motion and the formation of the ligaments as a consequence of the primary break-up.

The evolution of the jet at various axial distances from the discharge hole has been monitored in terms of the non-dimensional external liquid edge radius and non-dimensional film thickness extracted from the numerical simulation for the test case # 1 of Table 1. The two graphs of Figure 5 show the two non-dimensional jet profiles, evidencing that, as the jet penetrates, the external radius of the liquid umbrella increases, while the liquid film thickness reduces, as expected. The figure also reports the results from the analytical model of Nonnenmacher and Piesche [12], previously validated against experimental data, showing a good agreement between the numerical predictions and the analytical model. The same results were obtained for the test case # 2 of Table 1 (not shown), suggesting that the numerical model correctly catches the jet development in the region where the jet break-up is expected to occur.

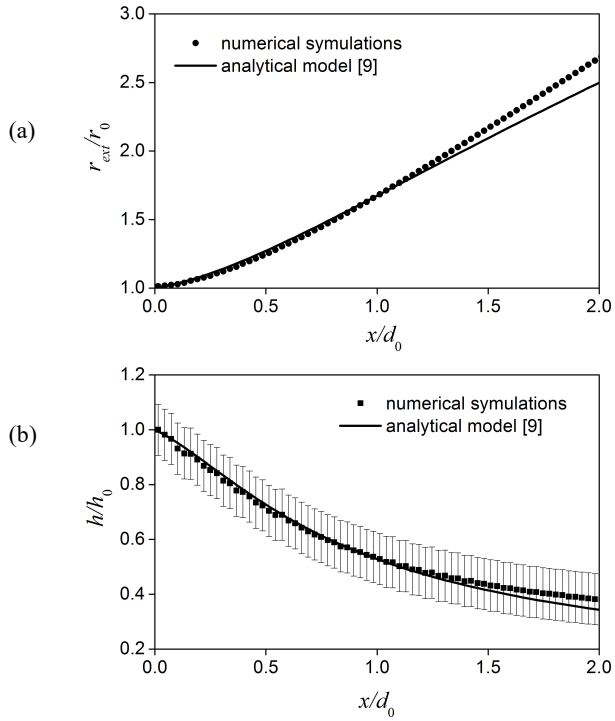

Figure 5: (a) Jet profile along the axial direction and (b) non-dimensional film thickness (error bars due to grid cell size are reported) as predicted by numerical simulations and by the analytical model [12], for the test case #1 listed in **Table 1**.

3.1. Jet instability propagation

The break-up of the liquid jet exiting the nozzle is caused by the unstable growth of disturbances on the jet surface, due to the aerodynamic interaction between the liquid jet and the environmental gas (Kelvin-Helmoltz instability). Among the spectrum of wavelengths characterising the disturbance, the fastest growing wave is the one that is directly responsible of the liquid jet rupture and it can be visually detected in the simulation results, as shown in Figure 6.

The results evidence that the sinusoidal (anti-symmetric) wave is responsible of the jet break-up, while no evidence of varicose (symmetric) wave is found, in accordance with the theoretical predictions for these operating conditions [2]. From the extracted data, it is possible to measure the wavelength of the fastest growing disturbance, as evidenced also in Figure 6.

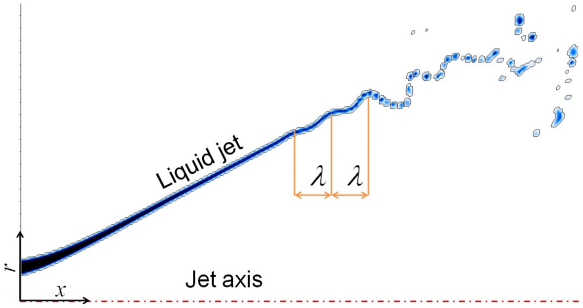

Figure 6: Jet profile extracted from numerical simulations, showing the sinusoidal instability that causes the jet break-up.

Table 2 reports, for both test cases of Table 1, the values of wavelength and corresponding frequency as extracted from the numerical simulations and predicted by the well-known model of Senecal et al. [2], based on linear instability analysis and extending the model of [13] to viscous conditions. The wavelengths predicted by the numerical simulations are much larger than those predicted by the linear stability theory, suggesting that further analysis is needed both in the DNS and analytical approaches.

Variable	Model	Case # 1	Case # 2
λ [μm]	Numerical simulation	245.5	264.5
	Analytical model [1]	35.9	51.1
L_b/d_0	Numerical simulation	3.569	3.843
	Analytical model [1]	1.648	3.195

Table 2: wavelength (λ) of the fastest growing disturbance and jet break-up length (L_b) non-dimensionalised by the discharge hole diameter.

3.2. Jet break-up

The previously described instability propagation is responsible of the jet break-up, as can be appreciated by the graph reported in Figure 6, and the size of the liquid lamella at the break-up point defines the size of the liquid ligaments.
The distance along the axial direction from the nozzle exit is called break-up length (L_b) and it is an important parameter in many primary atomisation models used in CFD code for spray investigation.
The break-up lengths extracted from the numerical simulations following the method suggested by [14], for both test cases of Table 1, are also reported in Table 2 together with the predictions from the analytical model [2]. The rather significant discrepancies should be associated to some peculiarity of the complex phenomena taking place during the lamella disruption.
One of the reasons could possibly be connected to the features of the air flow around the break-up region. Figure 7 shows the existence of a gas vortical structure close to the jet tip, which appears to strongly interact with the liquid lamella. These findings reveal the existence of macroscopic aerodynamic effects that clearly cannot be accounted for by simplified analytical models, based on Kelvin-Helmoltz instability analysis. This suggests that further investigation is necessary to fully understand the complex gas/liquid interaction phenomena and its effect on the jet stability and break-up.

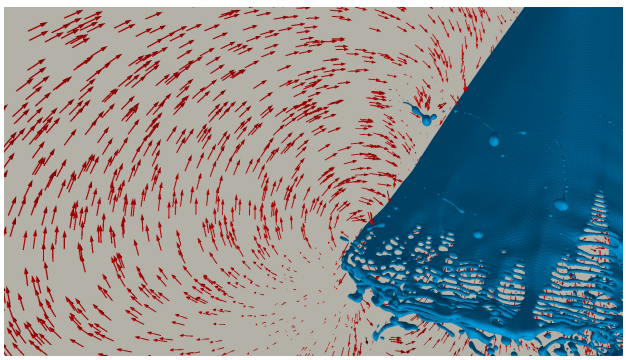

Figure 7: Gas flow field around the jet tip.

3.3. Characteristics of liquid ligaments

The lamella break-up produces liquid structures that are usually far to be spherical, see figure 4, quite the opposite of what usually figured in the common description of primary break-up. Highly deformed liquid ligaments are generally not detected by experimental techniques like Phase Doppler Anemometry or diffraction particle sizing, which assume spherical shapes of the measured drops. To classify the shape of a ligament predicted by the numerical simulation the following procedure was applied: the maximum (L_1) and the minimum (L_2) distances of the surface from the centre of mass of the liquid structure were evaluated (see figure 8), then the aspect ratio of the ligament was defined as the ratio $AR=L_1/L_2>1$.
To perform a significant statistics of the ligament population, a plane normal to the jet axis was chosen and only those liquid structures that cross this plane over a given time interval are considered.

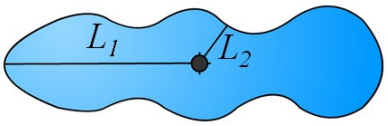

Figure 8: Sketch of ligament shape and characteristic lengths.

The time interval between 0.23ms to 0.43ms after start of injection was chosen in order to analyse a quasi steady-state regime. A nominal ligament size can be defined by the volume diameter defined as:

$$d_{Vol} = \sqrt[3]{\frac{6V}{\pi}} \tag{5}$$

where V is the ligament volume. Figure 9 shows, for case #1, the ligament nominal size distribution evaluated over different samples of the above described population: each curve represents the distribution calculated over the sample with AR lower than a given threshold. A similar result was obtained for case #2.

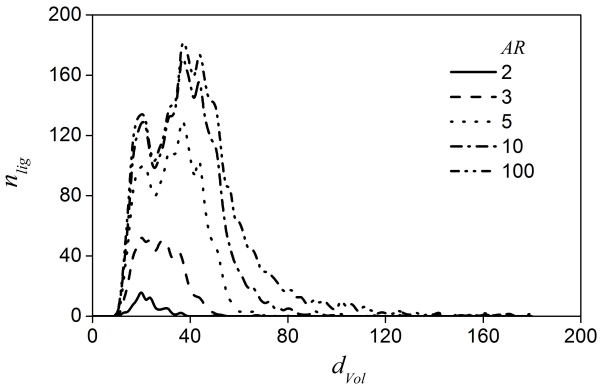

Figure 9: Ligament size distribution for different populations of ligament shapes; case #1 of **Table 1**.

Two features of this figure are noteworthy. First, the amount of ligaments with aspect ratio lower than 2 is quite small, and even smaller is the amount of ligaments having AR closer to 1 (e.g.

spherical drops), showing that during primary atomisation spherical drops must be very rare. Second, the shape of the distribution does not significantly change for *AR* larger than 5, meaning that for highly deformed ligaments, the size distribution does not depend on the shape.
Figure 10 shows volume and number cumulative distributions of the aspect ratio for the two test cases of table 1. The number distribution evidences that 90% of the ligaments have *AR* lower then 10, while the volume distribution reveals that the 90% of the total volume belongs to ligaments with *AR* lower than 40. This means that a relatively small number of highly deformed ligaments (*AR*>10) contains a significant amount of liquid, confirming that after primary atomisation the liquid structure cannot be described as spherical drops.

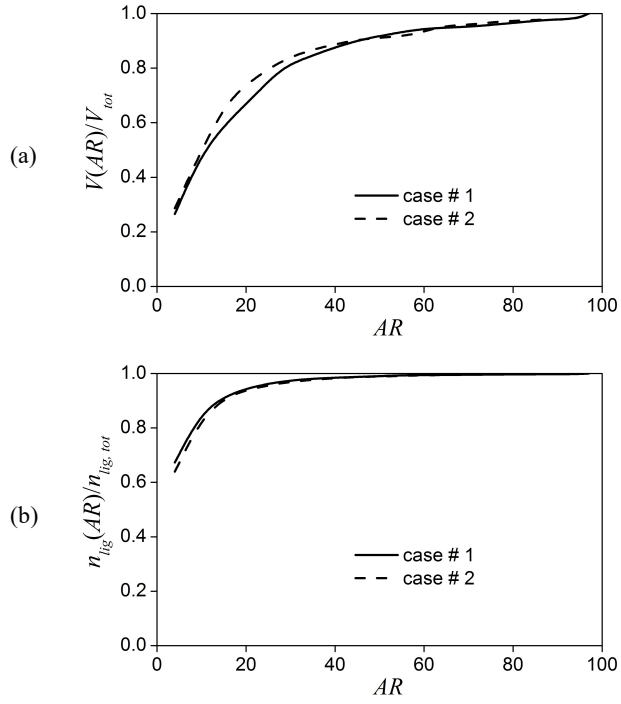

Figure 10: (a) Volume and (b) number of liquid structures at different *AR* values.

4. Conclusions

Multiphase DNS investigations of a conical swirled jet have been performed with the aim of identifying the most important aspects of the jet break-up. Two operating conditions have been investigated, characterized by two different gas density (13.3kg/m^3 and 6.8kg/m^3) to evidence the effect of aerodynamic interactions on the jet evolution and break-up.
The propagation of the conical lamella instabilities have been analysed showing the absence of a varicose mode and quantifying the fastest growing disturbance wavelength and the jet break-up length. Comparison with classical models shows rather significant discrepancies, which can be partially attributed to the complex aerodynamic interaction around the break-up region, that cannot be caught by the classical analysis based on Kelvin-Helmholtz instability.
The break-up outcomes mainly consist of highly deformed ligaments, quite the opposite of what generally figured in the common description of primary break-up where spherical droplets are the expected outcomes. A quantitative analysis shows that a relative small number of highly deformed ligaments contain a considerable amount of the total atomised mass.

5. Nomenclature

Latin symbols

AR	-	aspect ratio
d	m	diameter
f_σ	kg/(m^{2}s^2)	surface tension volume force
g	m/s^2	gravitational acceleration
h	m	lamella half-thickness
KF	-	Kolmogorov factor
L_1, L_2	m	ligament main dimensions
L_b	m	break-up length
L_t	m	macro-scale turbulence length
$\dot{m}_l$	kg/s	mass flow rate
n	-	counts
p	Pa	pressure
r	m	radial coordinate
r_0	m	nozzle radius
Re_t	-	turbulence Reynolds number
S	Pa	shear stress tensor.
t	s	time
u	m/s	velocity vector
u'	m/s	velocity turbulent fluctuation
V	m^3	volume
x	m	axial coordinate

Greek symbols

λ	m	wavelength
λ_k	m	Kolmogorov length scale
ρ	kg/m^3	density
μ	kg/(ms)	dynamic viscosity

Sub-scripts

g	-	gas
l	-	liquid
lig	-	ligament
Vol	-	volume

References

[1] Lefebvre, A., 1989, Atomization and sprays, CRC press.
[2] Senecal, P. K., Schmidt, D. P., Nouar, I., Rutland, C. J., Reitz, R. D., and Corradini, M. L., 1999, "Modeling high-speed viscous liquid sheet atomization," International Journal of Multiphase Flow, 25(6), pp. 1073-1097.
[3] Panchagnula, M. V., Sojka, P. E., and Santangelo, P. J., 1996, "On the three dimensional instability of a swirling, annular, inviscid liquid sheet subject to unequal gas velocities," Physics of Fluids, 8(12), pp. 3300-3312.
[4] Sirignano, W. A., and Mehring, C., 2000, "Review of theory of distortion and disintegration of liquid streams," Progress in Energy and Combustion Science, 26(4), pp. 609-655.
[5] Bode, M., Diewald, D., Broll, D. O., F. Heyse, J. F., Le Chedanec, V., and Pitsch, H., 2014, "Influence of the injector

geometry on primary breakup in Diesel injector systems," SAE Technical Paper Series 2014-01-142.
[6] Gomaa, H., Kumar, S., Huber, C., Weigand, B., and Peters, B., "Numerical comparison of 3D jet breakup using a compression scheme and an interface reconstruction based VOF code," Proc. 24th ILASS Europe Conference.
[7] Shinjo, J., and Umemura, A., 2011, "Surface instability and primary atomization characteristics of straight liquid jet sprays," Int. J. Multiphase Flows, 37, pp. 1294-1304.
[8] Sander, W., and Weigand, B., 2008, "Direct numerical simulation and analysis of instability enhancing parameters in liquid sheets at moderate Reynolds numbers," Physics of Fluids, 20(5), p. 053301.
[9] Eisenschmidt, K., Ertl, M., Gomaa, H., Kieffer-Roth, C., Meister, C., Rauschenberger, P., Reitzle, M., Schlottke, K., and Weigand, B., 2015, "Direct numerical simulations for multiphase flows: An overview of the multiphase code FS3D," Applied Mathematics and Computation, 272, pp. 508-517.
[10] Galbiati, C., Ertl, M., Tonini, S., Cossali, G. E., and Weigand, B., 2015, "DNS Investigation of the Primary Breakup in a Conical Swirled Jet," High Performance Computing in Science and Engineering '15, Springer, pp. 333-347.
[11] Galbiati, C., Tonini, S., Conti, P., and Cossali, G. E., 2016, "Numerical simulations of internal nozzle flow in a pressure swirl atomizer for aircraft engines," submitted to Journal of Propulsion and Power.
[12] Nonnenmacher, S., and Piesche, M., 2000, "Design of hollow cone pressure swirl nozzles to atomize Newtonian fluids," Chemical Engineering Science, 55(19), pp. 4339-4348.
[13] Reitz, R. D., and Bracco, F. V., 1986, "Mechanisms of breakup of round liquid jets," Encyclopedia of fluid mechanics, 3, pp. 233-249.
[14] Dumouchel, C., Cousin, J., and Triballier, K., 2005, "Experimental analysis of liquid-gas interface at low Weber number: interface length and fractal dimension," Experiments in fluids, 39(4), pp. 651-666.